Effect of Gd Substitution on the Structural, Morphological, and Optical Properties of $Y_3Fe_5O_{12}$ Nanoparticles

Shaikh Taufiq Khalil Ahemad[1], Samyak M. Bansode[1], Devendra D. Narwade[1], Yogesh B. Adsul[1], Vishaljyot R. Divekar[1], V. D. Murumkar[2]

[1]*Department of Physics, Deogiri College, Aurangabad, India*
[2]*Department of Physics, Vivekanand Arts, Sardar Dalipsingh commerce and science college, India.*

Abstract: In this study, $Y_{3-x}Gd_xFe_5O_{12}$ (x = 0.0 and x = 0.4) nanoparticles were synthesized and characterized to examine the influence of Gd substitution on their structural, morphological, and optical properties. X-ray diffraction (XRD) analysis confirmed the formation of a garnet structure with an increase in lattice parameter due to Gd incorporation. Fourier Transform Infrared (FTIR) spectroscopy identified Fe–O and Y–O/Gd–O stretching vibrations, indicating structural modifications. Scanning Electron Microscopy (SEM) revealed a quasi-spherical morphology with increased particle size and enhanced agglomeration in the Gd-doped sample. UV-Vis spectroscopy demonstrated strong absorption in the UV and visible regions, with a red shift in the absorption edge upon Gd substitution. The results suggest that Gd incorporation alters the microstructure and optical behaviour of YIG, making it a promising candidate for magneto-optical and optoelectronic applications.

Keywords: Yttrium Iron Garnet (YIG), Gadolinium Substitution, XRD, FTIR, SEM, UV

1. Introduction

Yttrium iron garnet ($Y_3Fe_5O_{12}$, YIG) is a significant material in the fields of magnetism, electronics, and optics, owing to its unique structural, dielectric, and magnetic properties. YIG garnets belong to the family of ferrites that crystallize in a cubic structure and are widely used in microwave communication, magnetic sensors, magneto-optical devices, and optical coatings. These materials exhibit low electrical conductivity and high resistivity, making them suitable for applications where low energy losses are required. The introduction of dopants into the YIG structure has been extensively explored to tailor its electrical, magnetic, and optical properties for advanced technological applications [1]. Gadolinium (Gd^{3+}) doping in YIG has garnered attention due to the larger ionic radius of Gd^{3+} compared to Y^{3+}, which alters the crystal structure, modifies lattice parameters, and influences the magnetic and dielectric behaviour. The substitution of Gd^{3+} in YIG is expected to induce significant changes in dielectric properties, AC conductivity, and optical band gap due to modifications in electron-lattice interactions and local distortions in the garnet structure [2]. The effect of Gd^{3+} doping on the dielectric response and optical properties is crucial in determining its potential for high-frequency applications, microwave absorption, and optical filters. The primary objective of this study is to synthesize $Y_{3-x}Gd_xFe_5O_{12}$ (x = 0.0 and 0.4) nanoparticles using the sol-gel method and investigate the impact of Gd^{3+} incorporation on the structural, dielectric, and optical properties. The synthesized samples will be characterized using X-ray diffraction (XRD) for phase confirmation, Fourier transform infrared spectroscopy (FTIR) for functional group analysis, dielectric measurements (two-probe technique) for frequency-dependent electrical properties, and UV-Vis spectroscopy for optical absorption and band gap analysis [3]. This study aims to provide insight into the structural modifications and potential applications of Gd^{3+}-substituted YIG nanoparticles in dielectric resonators, optical coatings, and high-frequency electronic devices.

2. Experimental

2.1 Materials

The raw materials used for the synthesis of $Y_{3-x}Gd_xFe_5O_{12}$ nanoparticles include yttrium nitrate [$Y(NO_3)_3$], gadolinium nitrate [$Gd(NO_3)_3$], and iron nitrate [$Fe(NO_3)_3$], all of which serve as precursors for the cationic components. Citric acid is used as a complexing agent to form metal-chelated precursors, ensuring homogeneity in the sol-gel process. Ammonia solution is employed for pH adjustment, promoting the controlled precipitation of the precursor gel. Ethanol and distilled water act as solvents to dissolve the precursors and facilitate uniform mixing of the reactants [4].

2.2 Synthesis by Sol-Gel Method

The sol-gel method is a widely used wet-chemical approach for the synthesis of nanoparticles with high purity and controlled stoichiometry. In this study, $Y_{3-x}Gd_xFe_5O_{12}$ nanoparticles were synthesized by dissolving $Y(NO_3)_3$, $Gd(NO_3)_3$, and $Fe(NO_3)_3$ in a mixture of ethanol and distilled water. Citric acid was then added as a chelating agent to form a stable metal-ion complex, ensuring uniform distribution of cations in the sol [5]. The solution was continuously stirred at room temperature, followed by the gradual addition of ammonia to adjust the pH to 7–8, promoting the formation of a homogeneous precursor gel. The resulting gel was dried at 120°C to remove excess moisture and organic residues [6]. The dried precursor was then calcined at an optimized temperature 800°C to promote crystallization and remove volatile organic components. The annealed samples were ground to obtain fine nanopowders of $Y_{3-x}Gd_xFe_5O_{12}$ (x = 0.0 and 0.4) for further characterization. The sol-gel approach ensures fine particle size, controlled morphology, and improved phase purity, making it a suitable technique for synthesizing Gd^{3+}-doped YIG nanoparticles.

3. Results and Discussion

3.1 X-ray Diffraction (XRD) Analysis

The X-ray diffraction (XRD) patterns of $Y_{3-x}Gd_xFe_5O_{12}$ nanoparticles with x = 0.0 and x = 0.4 confirm the formation of a garnet-type phase without any detectable secondary phases, indicating the successful incorporation of Gd^{3+} ions into the YIG lattice. The diffraction peaks match well with the standard JCPDS card for yttrium iron garnet (YIG), suggesting that the cubic garnet structure is retained even after Gd substitution [7]. The crystallite size (D) was estimated using the Scherrer equation, $D=k\lambda / \beta\cos\theta$, where k=0.9 is the Scherrer constant, λ=1.5406Å (Cu Kα radiation), β is the full width at half maximum (FWHM) in radians, and θ is the Bragg angle. The calculated average crystallite size was found to be 38.24 nm for $Y_3Fe_5O_{12}$ (x=0.0) and 35.18 nm for $Y_{2.6}Gd_{0.4}Fe_5O_{12}$ (x=0.4). The slight decrease in crystallite size upon Gd substitution may be attributed to lattice distortion caused by the difference in ionic radii between Y^{3+} (0.90 Å) and Gd^{3+} (0.94 Å).

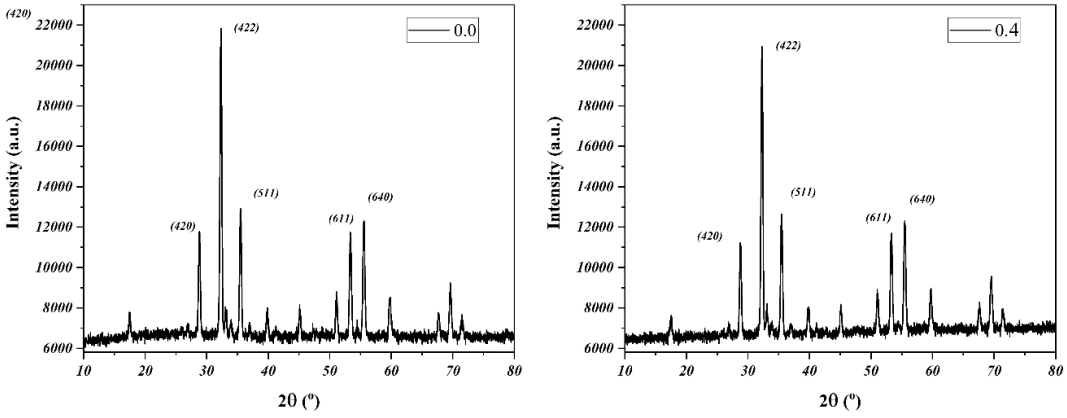

Figure 1: XRD pattern of $Y_3Fe_5O_{12}$ (x = 0.0, 0.4) nanoparticles

The lattice parameter (a) was determined assuming a cubic crystal structure using the relation: $a=d\sqrt{h2+k2+l2}$, where d is the interplanar spacing, and (hkl) are the Miller indices of the diffraction planes

[8]. The calculated lattice parameter was found to be 12.376 Å for x = 0.0 and 12.421 Å for x = 0.4, showing a slight increase with Gd substitution, which is expected due to the larger ionic radius of Gd^{3+}. The microstrain (ε) was estimated using the equation, $\varepsilon = \beta / 4\tan\theta$, The calculated values of microstrain were 2.12×10^{-3} for x = 0.0 and 2.47×10^{-3} for x = 0.4, indicating a slight increase in internal strain with Gd substitution.
The dislocation density (δ) was calculated using: $\delta = 1 / D2$, the values obtained were 6.84×10^{12} nm^{-2} for x = 0.0 and 8.08×10^{12} nm^{-2} for x = 0.4, indicating an increase in defects with Gd doping. The unit cell volume (v) was calculated using: $V = a3$. The values obtained were 1897.56 $Å^3$ for x = 0.0 and 1914.83 $Å^3$ for x = 0.4, confirming the expansion of the unit cell due to Gd substitution. These results confirm that Gd doping influences the structural properties of YIG, leading to changes in crystallite size, lattice parameters, strain, and density, which may impact its magnetic and dielectric properties [9].

3.2 Fourier Transform Infrared (FTIR) Spectroscopy Analysis
The FTIR spectra of $Y_{3-x}Gd_xFe_5O_{12}$ nanoparticles (x = 0.0 and x = 0.4) were recorded in the range of 1000–400 cm^{-1} to examine the vibrational modes of metal-oxygen bonds and confirm the garnet phase formation.

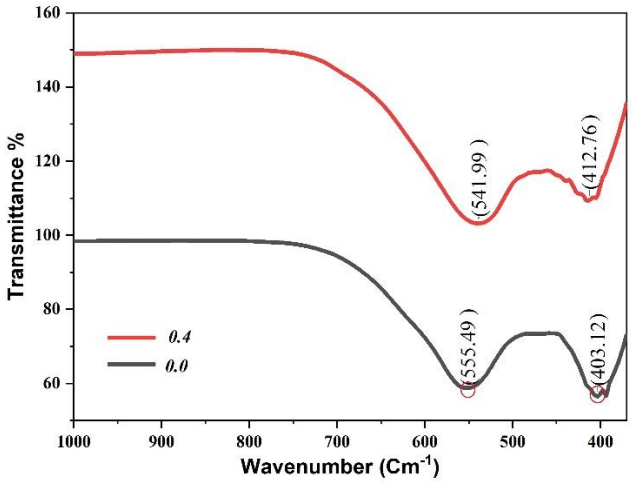

Figure 2 : FTIR spectra of $Y_{3-x}Gd_xFe_5O_{12}$ (x = 0.0 and x = 0.4) nanoparticles
The spectra exhibit characteristic absorption bands associated with Fe–O and Y–O/Gd–O stretching vibrations, indicating structural integrity and modifications upon Gd substitution [10] [6]. A prominent absorption peak is observed at 555.49 cm^{-1} for the x = 0.0 sample, corresponding to Fe–O stretching vibrations in the tetrahedral coordination, which slightly shifts to 541.99 cm^{-1} in the x = 0.4 sample, suggesting changes in the Fe–O bond strength due to the incorporation of Gd^{3+} ions.
Similarly, the Y–O vibration in the octahedral coordination, observed at 403.12 cm^{-1} for x = 0.0, shifts to 412.76 cm^{-1} for x = 0.4, confirming the successful substitution of Y^{3+} by larger Gd^{3+} ions. The shifts in vibrational frequencies indicate lattice distortions due to ionic size differences, further supporting the structural modifications observed in the XRD analysis [11].

3.3 Scanning Electron Microscopy (SEM) Analysis
The SEM micrographs of $Y_{3-x}Gd_xFe_5O_{12}$ nanoparticles with x = 0.0 and x = 0.4 reveal significant insights into the morphological characteristics and particle size distribution of the synthesized samples [12].

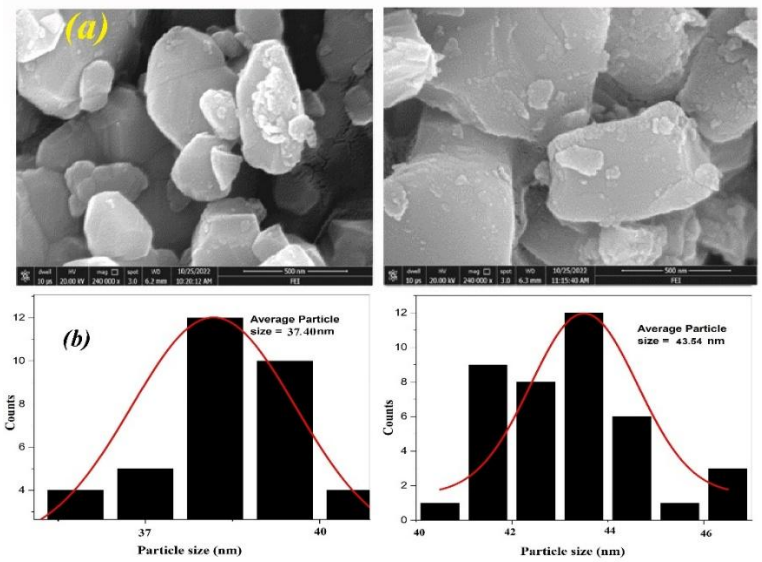

Figure 3 : SEM micrograph of Gd doped YIG NPs

Both samples exhibit a quasi-spherical to irregular polygonal morphology, which is commonly observed in yttrium iron garnet (YIG) nanoparticles synthesized via wet chemical methods. The presence of agglomerated grains suggests strong magnetic interactions among the nanoparticles, leading to the formation of dense structures [13].

The particle size distribution analysis, derived from the histogram, indicates an average particle size of 37.40 nm for x = 0.0 and 43.54 nm for x = 0.4. The slight increase in particle size upon Gd substitution can be attributed to the larger ionic radius of Gd^{3+} (0.94 Å) compared to Y^{3+} (0.90 Å), which causes a lattice expansion and promotes grain growth [14]. The micrographs also show that the degree of agglomeration increases with Gd doping, likely due to enhanced dipole-dipole interactions and modified magnetic properties of the substituted garnet structure [15].

Additionally, the SEM images reveal that the nanoparticles are densely packed with minimal porosity, indicating a high degree of sintering and effective growth control during synthesis. The uniform grain size distribution further supports the controlled nucleation and crystallization process [16]. The observed increase in particle size is in agreement with the XRD-derived crystallite size, confirming the successful incorporation of Gd^{3+} into the YIG lattice without altering the fundamental crystal structure [17].

3.4 UV-Vis Spectroscopy Analysis

The UV-Vis absorption spectra of $Y_{3-x}Gd_xFe_5O_{12}$ nanoparticles with x = 0.0 and x = 0.4 were recorded in the wavelength range of 200–1100 nm to investigate their optical absorption behavior.

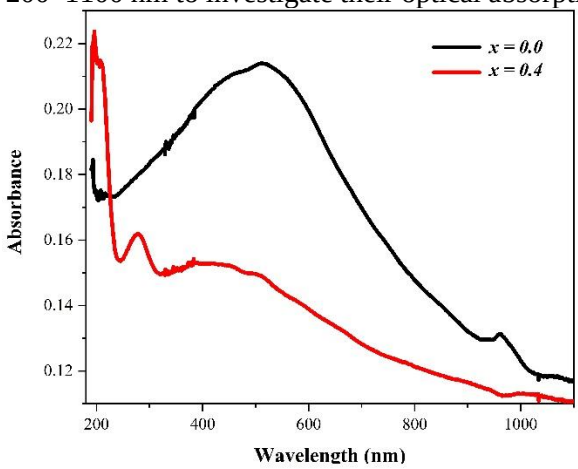

Figure 4: UV-Vis absorption spectra of $Y_{3-x}Gd_xFe_5O_{12}$ (x = 0.0 and x = 0.4) nanoparticles

The spectra exhibit strong absorption in the UV and visible regions, confirming the semiconductor-like nature of the synthesized materials [18]. The absorption intensity is higher for the x = 0.0 sample

compared to the x = 0.4 sample, which suggests that Gd substitution influences the optical response of the material.

A noticeable shift in the absorption edge is observed upon Gd doping, with the x = 0.4 sample showing absorption at longer wavelengths compared to the undoped sample (x = 0.0). This red shift in the absorption spectra may be attributed to lattice modifications and electronic interactions between Fe^{3+} and Gd^{3+} ions, which alter the optical transitions within the material [19]. Additionally, the absorption spectra show a broader range of absorption for the Gd-doped sample, indicating changes in the crystal field interactions and electronic structure [20].

4. Conclusion

The present study successfully synthesized and characterized $Y_{3-x}Gd_xFe_5O_{12}$ (x = 0.0 and x = 0.4) nanoparticles to investigate the effects of Gd substitution on their structural, morphological, and optical properties. X-ray diffraction (XRD) analysis confirmed the formation of a single-phase garnet structure with an increase in lattice parameter upon Gd doping, indicating the successful incorporation of Gd^{3+} ions into the YIG lattice. The calculated crystallite size decreased slightly with Gd substitution, while the dislocation density and microstrain increased, suggesting minor lattice distortions due to ionic size differences. Fourier Transform Infrared (FTIR) spectroscopy validated the presence of characteristic Fe–O stretching and Y–O/Gd–O vibrations, with peak shifts confirming the structural modifications induced by Gd doping. Scanning Electron Microscopy (SEM) analysis revealed a quasi-spherical to polygonal morphology with an increase in average particle size from 37.40 nm (x = 0.0) to 43.54 nm (x = 0.4), supporting the lattice expansion observed in XRD. The micrographs also indicated enhanced agglomeration in the Gd-doped sample, likely due to stronger magnetic interactions. UV-Vis absorption spectroscopy demonstrated strong absorption in the UV and visible regions, with a red shift in the absorption edge upon Gd substitution. This shift suggests that Gd incorporation affects the optical properties of YIG by modifying electronic interactions within the material.

References

1. M. Shkir, K. Chandekar, A. Khan, … A. E.-T.-M. C. and, and undefined 2020, "Structural, morphological, vibrational, optical, and nonlinear characteristics of spray pyrolyzed CdS thin films: effect of Gd doping content," Elsevier, Accessed: Mar. 12, 2025. [Online]. Available: https://www.sciencedirect.com/science/article/pii/S0254058420309779
2. C. Murugesan, G. C.-R. advances, and undefined 2015, "Impact of Gd 3+ substitution on the structural, magnetic and electrical properties of cobalt ferrite nanoparticles," pubs.rsc.org, Accessed: Mar. 12, 2025. [Online]. Available: https://pubs.rsc.org/en/content/articlehtml/2015/ra/c5ra14351a
3. A. Sharma, H. S.-J. of M. S. M. in, and undefined 2021, "Influence of Gd doping and thickness variation on structural, morphological and optical properties of nanocrystalline bismuth ferrite thin films via sol–gel technology," Springer, Accessed: Mar. 12, 2025. [Online]. Available: https://link.springer.com/article/10.1007/s10854-021-06571-5
4. N. Tian, Y. Zhang, H. Huang, … Y. H.-T. J. of P., and undefined 2014, "Influences of Gd Substitution on the Crystal Structure and Visible-Light-Driven Photocatalytic Performance of Bi2WO6," ACS Publications, Accessed: Mar. 12, 2025. [Online]. Available: https://pubs.acs.org/doi/abs/10.1021/jp500645p
5. S. Manwar, A. Ingle, … V. P.-…-A. Q. J., and undefined 2023, "Green synthesis of co-doped zns thin films using ethanol," indianjournals.comSA Manwar, AG Ingle, VA Pandit, VK Kashte, NN KapseBIOINFOLET-A Quarterly Journal of Life Sciences, 2023•indianjournals.com, Accessed: Mar. 12, 2025. [Online]. Available: https://www.indianjournals.com/ijor.aspx?target=ijor:bil&volume=20&issue=3a&article=019
6. V. A. Pandit, N. N. Kapse, V. K. Kashte, and N. D. Chaudhari, "Study on the green synthesis and characterization of Co2+ doped Mg–Zn ferrite nanoparticles using orange juice extract," Appl Phys A Mater Sci Process, vol. 130, no. 12, Dec. 2024, doi: 10.1007/S00339-024-07987-6.
7. M. F. Sarac, "Magnetic, Structural, and Optical Properties of Gadolinium-Substituted Co0.5Ni0.5Fe2O4 Spinel Ferrite Nanostructures," J Supercond Nov Magn, vol. 33, no. 2, pp. 397–406, Feb. 2020, doi: 10.1007/S10948-019-05359-3.
8. A. D. Sharma and H. B. Sharma, "Influence of Gd doping and thickness variation on structural, morphological and optical properties of nanocrystalline bismuth ferrite thin films via sol–gel technology," Journal of Materials Science: Materials in Electronics, vol. 32, no. 15, pp. 20612–20624, Aug. 2021, doi: 10.1007/S10854-021-06571-5.

9. M. Akhtar, A. Sulong, M. Ahmad, … M. K.-J. of A. and, and undefined 2016, "Impacts of Gd–Ce on the structural, morphological and magnetic properties of garnet nanocrystalline ferrites synthesized via sol–gel route," Elsevier, Accessed: Mar. 12, 2025. [Online]. Available: https://www.sciencedirect.com/science/article/pii/S0925838815317023
10. D. Mithal, T. K.-S. S. Sciences, and undefined 2017, "Effect of Gd3+ doping on structural and optical properties of ZnO nanocrystals," Elsevier, Accessed: Mar. 12, 2025. [Online]. Available: https://www.sciencedirect.com/science/article/pii/S129325581730105X
11. V. K. Kashte, V. A. Pandit, N. N. Kapse, D. Rathod, and B. G. Toksha, "Effect of Al3+ Doping on the Microstructure and Magnetic Behavior of CoFe2O4 Nanoparticles," J Supercond Nov Magn, vol. 38, no. 1, Feb. 2025, doi: 10.1007/S10948-024-06892-6.
12. M. Mazhdi and M. J. Tafreshi, "The effects of gadolinium doping on the structural, morphological, optical, and photoluminescence properties of zinc oxide nanoparticles prepared by co-precipitation method," Appl Phys A Mater Sci Process, vol. 124, no. 12, Dec. 2018, doi: 10.1007/S00339-018-2291-0.
13. R. Jogdand, V. Pandit, … J. B.-…-A. Q. J., and undefined 2023, "Green Synthesis, Characterization and Antimicrobial Characters of Zinc Sulfide Nanoparticles," indianjournals.comRS Jogdand, VA Pandit, JV Bharad, AD ChapolikarBIOINFOLET-A Quarterly Journal of Life Sciences, 2023•indianjournals.com, Accessed: Mar. 12, 2025. [Online]. Available: https://www.indianjournals.com/ijor.aspx?target=ijor:bil&volume=20&issue=2a&article=002
14. S. Joshi, M. Kumar, S. Chhoker, … A. K.-J. of M. and, and undefined 2017, "Effect of Gd3+ substitution on structural, magnetic, dielectric and optical properties of nanocrystalline CoFe2O4," Elsevier, Accessed: Mar. 12, 2025. [Online]. Available: https://www.sciencedirect.com/science/article/pii/S0304885316317486
15. V. Pandit, K. Sature, … D. T.-…-A. Q. J., and undefined 2022, "Properties of cr doped NI-ZN ferrite nanoparticles synthesized using lemon juice," indianjournals.comVA Pandit, KR Sature, DP Thorat, RA Gaikwad, DM Sonawane, PP Raut, GM DharneBIOINFOLET-A Quarterly Journal of Life Sciences, 2022•indianjournals.com, Accessed: Mar. 12, 2025. [Online]. Available: https://www.indianjournals.com/ijor.aspx?target=ijor:bil&volume=19&issue=2&article=025
16. V. Pandit, N. Kapse, … V. K.-J. of M. and, and undefined 2024, "Magnetic Behaviour, and initial permeability of green synthesized Co2+ substituted Ni-Zn ferrite," ElsevierVA Pandit, NN Kapse, VK Kashte, ND ChaudhariJournal of Magnetism and Magnetic Materials, 2024•Elsevier, Accessed: Mar. 12, 2025. [Online]. Available: https://www.sciencedirect.com/science/article/pii/S030488532400475X
17. B. Poornaprakash, U. Chalapathi, … S. B.-P. E. L., and undefined 2017, "Structural, morphological, optical, and magnetic properties of Gd-doped and (Gd, Mn) co-doped ZnO nanoparticles," Elsevier, Accessed: Mar. 12, 2025. [Online]. Available: https://www.sciencedirect.com/science/article/pii/S1386947717303478
18. M. Mazhdi, M. T.-A. P. A, and undefined 2018, "The effects of gadolinium doping on the structural, morphological, optical, and photoluminescence properties of zinc oxide nanoparticles prepared by co-precipitation," Springer, Accessed: Mar. 12, 2025. [Online]. Available: https://link.springer.com/article/10.1007/s00339-018-2291-0
19. A. Kalam, A. Al-Sehemi, … M. A.-J. of I. and, and undefined 2023, "doped ZnO nanomaterials using the modified-solvothermal method and studied the effect of gadolinium on the structural, morphological, and optical properties," Springer, Accessed: Mar. 12, 2025. [Online]. Available: https://link.springer.com/article/10.1007/s10904-023-02745-2
20. M. Ansari, S. Khan, N. A.-J. of M. and Magnetic, and undefined 2018, "Effect of R3+ (R= Pr, Nd, Eu and Gd) substitution on the structural, electrical, magnetic and optical properties of Mn-ferrite nanoparticles," Elsevier, Accessed: Mar. 12, 2025. [Online]. Available: https://www.sciencedirect.com/science/article/pii/S0304885317338763